JTTEE5 17:805–811
DOI: 10.1007/s11666-008-9246-5
1059-9630/$19.00 © ASM International



# Development and Investigation on New Composite and Ceramic Coatings as Possible Abradable Seals

*U. Bardi, C. Giolli, A. Scrivani, G. Rizzi, F. Borgioli, A. Fossati, K. Partes, T. Seefeld, D. Sporer, and A. Refke*

*(Submitted June 25, 2008; in revised form August 18, 2008)*

**To improve gas turbine performance, it is possible to decrease back flow gases in the high-temperature combustion region of the turbo machine by reducing the shroud/rotor gap. Thick and porous thermal barrier coating (TBC) systems and composite CoNiCrAlY/$Al_2O_3$ coatings made by air plasma spray and composite NiCrAlY/graphite coatings made by laser cladding were studied as possible high-temperature abradable seal on shroud. Oxidation and thermal fatigue resistance of the coatings were assessed by means of isothermal and cyclic oxidation tests. Tested CoNiCrAlY/$Al_2O_3$ and NiCrAlY/graphite coatings after 1000 h at 1100 °C do not show noticeable microstructural modification. The oxidation resistance of the new composite coatings satisfied original equipment manufacturer (OEM) specifications. Thick and porous TBC systems passed the thermal fatigue test according to the considered OEM procedures. According to the OEM specifications for abradable coatings, the hardness evaluation suggests that these kinds of coatings must be used with abrasive-tipped blades. Thick and porous TBC coating has shown good abradability using tipped blades.**

**Keywords** abradable coatings, air plasma spray, laser cladding

## 1. Introduction

New generation of gas turbine engines concentrate on performance gains, in particular by developing new materials that allow operating under much more severe conditions: superalloys and protective coatings are a permanent field of interest for engine designers (Ref 1). Gas turbine efficiency can be improved by increasing working temperatures, and also by improving dynamic sealing between rotating and stationary parts. One type of improved sealing being incorporated into turbines is abradable seals, to reduce the blade-tip clearances. Abradable materials must be able to withstand high-temperature erosion and oxidation, as well as to provide easy and controlled abrasion (Ref 2). The locations of abradable coatings include seals over compressor blades and seals over unshrouded first stage turbine blades and shrouded second and third stage turbine blades for industrial gas turbines (Ref 3). The commercial abradable coatings for compressor shrouds consist of polymer, AlSi-Polymer, metal matrix with solid lubricant, and MCrAlY with polyester, which withstand temperatures lower than 900 °C; abradable coatings for turbine shrouds are produced by using MCrAlY with polyester and ceramics that withstand temperatures greater than 900 °C. This kind of high-temperature abradable coatings must be used with blades tipped with abrasive coatings (Ref 4).

This work is focused on the development of abradable coatings to be applied on the first stage of industrial land base gas turbines where the temperatures are at the highest (Ref 5) for this type of engine. Composite metal-ceramic coatings were developed to combine the high-temperature oxidation (HTO) resistance of ceramic materials with the good mechanical properties of metal alloys, which should avoid the problems related to ceramic brittleness. Composite CoNiCrAlY/$Al_2O_3$ coatings made by air plasma spray (APS) and composite NiCrAlY/Graphite coatings made by laser cladding were produced and tested as a possible high-temperature abradable seal on shroud. The ceramic filler particles embedded in the

This article is an invited paper selected from presentations at the 2008 International Thermal Spray Conference and has been expanded from the original presentation. It is simultaneously published in *Thermal Spray Crossing Borders, Proceedings of the 2008 International Thermal Spray Conference*, Maastricht, The Netherlands, June 2-4, 2008, Basil R. Marple, Margaret M. Hyland, Yuk-Chiu Lau, Chang-Jiu Li, Rogerio S. Lima, and Ghislain Montavon, Ed., ASM International, Materials Park, OH, 2008.

**U. Bardi**, Dipartimento di Chimica, Università di Firenze, Via della Lastruccia 3, Sesto Fiorentino, 50019 Firenze, Italy; **U. Bardi** and **C. Giolli**, Consorzio Interuniversitario Nazionale per la Scienza e Tecnologia dei Materiali (INSTM), via Benedetto Varchi 59, 50132 Firenze, Italy; **C. Giolli, A. Scrivani,** and **G. Rizzi**, Turbocoating S.p.A., via Mistrali 3, 43010 Rubbiano di Solignano, Italy; **F. Borgioli** and **A. Fossati**, Dipartimento di Ingegneria Civile, Università di Firenze, via S. Marta 3, 50139 Firenze, Italy; **K. Partes** and **T. Seefeld**, Bremer Institut für angewandte Strahltechnik BIAS, Klagenfurterstr. 2, 28359 Bremen, Germany; **D. Sporer**, Sulzer Metco (Canada) Inc., Wies 21a, 6677 Schattwald, Austria; and **A. Refke**, Sulzer Metco AG (Switzerland), Rigackerstr. 16, 5610 Wohlen, Switzerland. Contact e-mail: carlogiolli@turbocoating.it.

metal matrix should improve the abradability due to their brittleness as it occurs for metal matrix with solid lubricant (Ref 4). Thick and porous thermal barrier coating (TBC) systems were also produced by APS without using plastic filler (Ref 6, 7) in the sprayed powder. The oxidation resistance of composite coatings and thermal fatigue resistance of thick and porous TBC systems were assessed according to original engine manufacturer (OEM) specifications by means of isothermal and cyclic oxidation tests, and their abradability was evaluated.

## 2. Experimental

### 2.1 Materials and Deposition Process

Hastelloy X (HX) samples (Ni-22Cr-19Fe-9Mo-2Co-1W), in the form of metal squared substrates (25 × 25 mm; thickness: 3 mm), were coated by APS. AMDRY 995 (Co-32Ni-21Cr-8Al-0.5Y) and $Al_2O_3$ powders were used. In the first stage, plasma spray parameters were adapted to the CoNiCrAlY powder through preliminary tests to obtain an average and homogeneous porosity of the coating of 16%. The resulting coating hardness was found to be 86.5 ± 1.5 HR 15Y. In fact, it is believed that abradable coatings benefit by a fairly high porosity, but this point has to be balanced against oxidation resistance (Ref 8). By using these selected spraying parameters, further spraying tests with both alumina and CoNiCrAlY powders were carried out. In the first tests, finer alumina, with an average size of −22 + 5 μm, was sprayed with a CoNiCrAlY powder in the ratio of 40% by weight of ceramic (Sample 1). Another set of samples (Sample 2) was obtained by spraying a coarser alumina powder, with an average size of −90 + 45 μm, again with a proportion of 40 wt.% of ceramic. In a third set of samples (Sample 3), a spheroidical ceramic powder, with an average size of −90 + 45 μm, in the same ratio, was used in order to determine whether the powder shape affects the coating properties.

Squared substrates (25 × 25 mm; thickness: 3 mm) of HX were also coated with a mixture of NiCrAlY and Ni/Graphite powders by laser cladding. Gas atomized AMDRY 9625 (Ni-22Cr-10Al-1.0Y) powder was used with a grain size distribution of −75 + 45 μm. The grain size distribution of the Ni/Graphite (60/40) powder (Durabrade™ 2200) was −115 + 45 μm. The powders were mixed inline with an Y-connecter (Sample 4). The laser cladded surface was generated using a solid-state Nd:Yag laser ''Trumpf HL 4006 D'' with a maximum output power of 4 kW. Powder was applied by a pneumatic powder feeding device in combination with an off axial nozzle. The laser power was 1200 W and the scan velocity was 1.2 m/min. The powder feed rate was 18 g/min for the MCrAlY and 2 g/min for the Ni/Graphite. The track offset was found to be optimal at 0.3 mm to realize the most constant clad height and a homogeneous dilution at the interface. The specimen (25 × 25 × 3 mm) was clad all over the upper (25 × 25 mm) surface.

A new APS process for making thick and porous TBC systems with a total thickness of up to 2 mm and a porosity level of the top coat of up to 30% without using plastic filler in the sprayed powder was developed (Ref 6). Three different kinds of TBC systems were coated by APS on circular substrates (diameter: 25 mm; thickness: 3 mm) of HX with the same bond coat of AMDRY 995 (average thickness of 250 μm) and with a top coat of yttria partially stabilized zirconia powder (Amperit 827.7 produced by H.C. Starck) (average thickness of about 1.8 mm) and low (17 ± 1%) (Sample 5), medium (21 ± 1%) (Sample 6), and high (29 ± 1%) (Sample 7) porosity levels of the top coat as described in previous papers [6, 7].

### 2.2 High-Temperature Oxidation Test and Furnace Cycling Test

The HTO tests were carried out in a Carbolite furnace (model CWF 13/5) with a maximum operating temperature of 1300 °C and a heating rate of 15 °C/min. Isothermal oxidation tests were performed at 1100 °C for 300 and 1000 h. Furnace cycle tests (FCTs) were performed using a test equipment consisting of an isothermal static air furnace (type: 3 zone split tube; $T_{max}$: 1300 °C), a specimen tray in Hastelloy X positioned on a vertical elevator, and a circular tube for the forced cooling of specimens when the elevator is lowered. Each thermal cycle in the FCT consisted of a 5-min heat up to the steady-state temperature, a 45-min soak at the steady-state temperature, and a 10-min forced air cool down. According to the OEM specifications, the chosen steady-state temperature was 1150 °C (Ref 5), and the minimum requested number of thermal cycles to pass the thermal cycling fatigue test was 250.

### 2.3 Microstructural and Phase Analysis

Samples before and after the oxidation tests were prepared for micrographic investigations by vacuum impregnation with epoxy, and then sectioned, ground, and finely polished (Ref 9). Microscopy analysis was performed by means of a metallographic optical microscope Zeiss Axiovert 100A with an image analyzer based on gray contrast, to determine powder morphology, coating microstructure, coating thickness, and coating porosity. Micrographic examinations and microprobe analysis were performed by ESEM QUANTA 200 FEI with EDAX-ZAF Quantification (Standardless).

X-ray diffraction analysis was performed by means of a Philips PW1050/37 diffractometer in Bragg-Brentano configuration (Cu Kα radiation generated at 40 kV and 25 mA). Diffraction patterns were analyzed by means of the program MAUD using the Rietveld method (Ref 10).

### 2.4 Hardness and Abradability Tests

Coating hardness was measured on a HR 15Y scale with a 12.5 mm steel ball and 15 kg major load. Before performing the tests, the coatings were carefully hand sanded with 60-grit SiC paper. According to the OEM specifications for abradable coatings, the recommended hardness

must be about 55-65 HR 15Y (for use with untipped blades) and 90-95 HR 15Y (for use with abrasive-tipped blades).

AISI 304 stainless steel samples (35 × 100 × 4 mm) were coated with the studied systems all over one 35 × 100 mm surface to be used as samples for abradability rig testing. In the function of the incursion rate, the test can last between 0.5 s and 10 min. So, it is possible to use stainless steel samples instead of nickel superalloy because this does not affect the test results (Ref 11). The tests were performed according to Sulzer Metco specifications. The rig consisted of a rotor, a movable specimen stage, and a heating device as shown in Fig. 1.

The infrastructure of the test equipment is similar to a large turbine balancing facility. For the high-temperature blade tests, a nickel superalloy disc was employed. The disc had 60 blade slots, 4 of which were furnished with a special attachment for dummy blades. Tipped c-BN and untipped dummy blades were used for the tests. The blade mass determines the maximum attainable blade tip velocity. Blade tip velocities up to 420 m/s were possible with Sulzer dummy blades. The blade tip velocities used were 250, 350, and 410 m/s (Ref 5, 11). All tests were conducted with an incursion rate in a range of 5-500 μm/s (Ref 5, 11).

The shroud specimen surfaces were heated by means of a high-velocity burner. A thermal gradient similar to that present in an engine was attained. The test temperature was about 1100 °C. The abradable specimen has fine thermocouples immediately below the surface to ensure that abradable surface temperature, and not flame radiation effects, is recorded. The thermocouples lie on the center line forming a cross. The blade height change was measured using a jig, which allowed the measurement of the blade height from a reference point. The jig was rigged with a digital micrometer. The setup was calibrated with a premeasured calibration blade prior to each measurement series. The measurement error was lower than 2 μm. The blade wear was evaluated as a percentage of a total incursion. Positive values describe wear of the blade whereas negative ones show transfer from the shroud. Therefore, a value of 100 exhibits no incursion into the coating and the total blade wear; on the other hand, a value of 0 indicates 100% incursion into the coating without any blade wear. The test conditions are reported in Table 1 for each kind of analyzed sample.

## 3. Results and Discussion

### 3.1 Coatings Characterization

Figure 2(a) shows the optical micrographs of a CoNiCrAlY coating sprayed with coarser alumina powders (Sample 1). Alumina is embedded in the metal matrix (30 ± 3% as evaluated by image analysis) as an interrupted layer. The alumina deposit between the passages of the torch is evident (dark lines). The different densities of the materials probably result in different behaviors during the flight in the plasma jet. Figure 2(b) shows the optical micrograph of a CoNiCrAlY coating sprayed with a finer alumina powder injected separately (Sample 2). These samples show a good homogeneity in the alumina distribution in the metal matrix in comparison to other samples. The alumina amount is lower in comparison with the other samples (22 ± 3%). Figure 2(c) shows the optical micrograph of a CoNiCrAlY coating sprayed with a spheroidical alumina powder (Sample 3). In this coating, alumina is grouped into clusters (30 ± 3%) and not uniformly dispersed in the metal matrix. Hardness values for all the samples are in a range of 84-98 HR 15Y. The presence of alumina resulted in a light increase of the

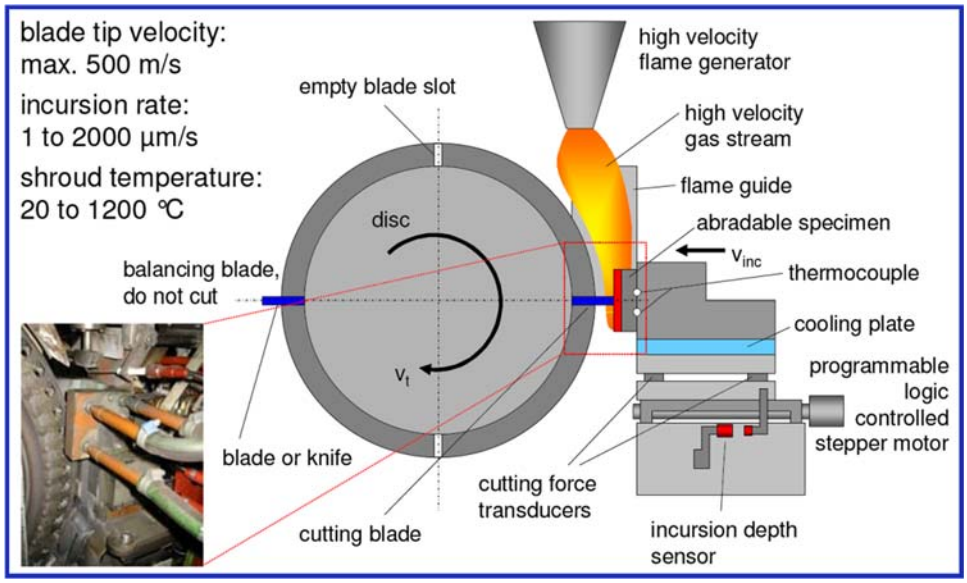


**Fig. 1** Schematic of the test rig for abradability testing

**Table 1 Abradability test conditions and results**

| Test No. | Abradable type | Remarks | Sample No. | Blade material and tipping | RPM | Velocity, m/s | Inc. rate, μm/s | Shroud wear track length, mm | Inc. depth, mm | Blade height change, mm | Total incursion depth, mm | Blade wear as % of incursion |
|---|---|---|---|---|---|---|---|---|---|---|---|---|
| 1 | MCrAlY/Alumina | | 2 | IN718 none | 9912 | 410 | 5 | 10.0 | 0.032 | −0.41 | 0.442 | 92.8 |
| 2 | | | 2 | IN718 cBN | 9912 | 410 | 5 | 34.5 | 0.377 | −0.16 | 0.537 | 29.8 |
| 3 | | | 2 | IN718 cBN | 9912 | 410 | 500 | 42.0 | 0.559 | 0.08 | 0.559 | −14.3 |
| 4 | | | 2 | IN718 cBN | 8461 | 350 | 50 | 39.0 | 0.482 | −0.22 | 0.702 | 31.4 |
| 5 | MCrAlY/Graphite | | 4 | IN718 none | 9912 | 410 | 5 | 8.0 | 0.020 | −0.43 | 0.450 | 95.5 |
| 6 | | | 4 | IN718 cBN | 9912 | 410 | 5 | 50.0 | 0.792 | 0.05 | 0.792 | −6.3 |
| 7 | | | 4 | IN718 cBN | 9912 | 410 | 500 | 25.5 | 0.198 | −0.72 | 0.918 | 78.4 |
| 8 | | | 4 | IN718 cBN | 8461 | 350 | 50 | 27.0 | 0.231 | −0.04 | 0.271 | 14.8 |
| 9 | | | 4 | IN718 cBN | 6044 | 250 | 5 | 37.0 | 0.433 | −0.20 | 0.633 | 31.6 |
| 10 | Thick, porous TBC | Low porosity | 5 | IN718 cBN | 6044 | 250 | 5 | 27.0 | 0.231 | −0.70 | 0.931 | 75.2 |
| 11 | | | 5 | IN718 cBN | 8461 | 350 | 50 | 38.5 | 0.469 | −0.36 | 0.829 | 43.4 |
| 12 | | | 5 | IN718 cBN | 9912 | 410 | 500 | 34.0 | 0.366 | −0.49 | 0.856 | 57.2 |
| 13 | | Medium porosity | 6 | IN718 cBN | 6044 | 250 | 5 | 58.0 | 1.066 | −0.06 | 1.126 | 5.3 |
| 14 | | | 6 | IN718 cBN | 8461 | 350 | 50 | 51.5 | 0.840 | −0.01 | 0.850 | 1.2 |
| 15 | | | 6 | IN718 cBN | 9912 | 410 | 500 | 51.5 | 0.840 | −0.03 | 0.870 | 3.4 |
| 16 | | High porosity | 7 | IN718 cBN | 6044 | 250 | 5 | 42.0 | 0.559 | −0.03 | 0.589 | 5.1 |
| 17 | | | 7 | IN718 cBN | 8461 | 350 | 50 | 50.0 | 0.792 | −0.01 | 0.802 | 1.2 |
| 18 | | | 7 | IN718 cBN | 9912 | 410 | 500 | 51.0 | 0.824 | −0.01 | 0.834 | 1.2 |




**Fig. 2** Optical images of CoNiCrAlY coatings produced with coarser alumina (Sample 1, (a)), with finer alumina (Sample 2, (b)), and with spheroidical alumina powder (Sample 3, (c)) coated on the Hastelloy X substrates by APS

hardness, due to the embedding of the alumina in the metal matrix. Image analysis indicates that the porosity level is not higher than in the CoNiCrAlY coating without alumina. The average thickness of the manufactured

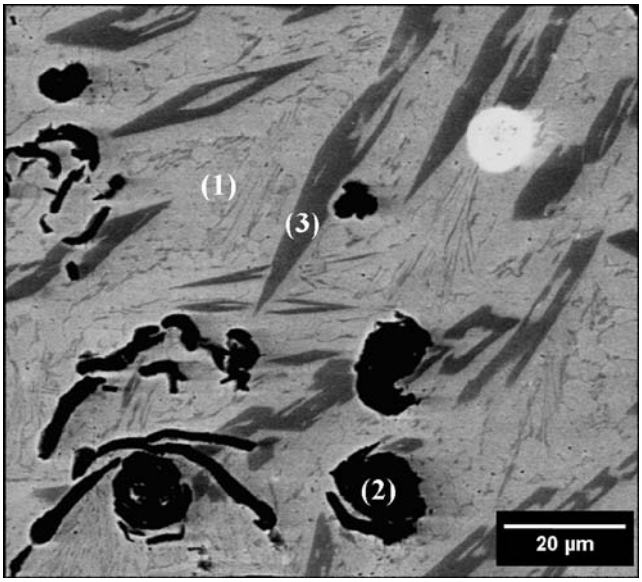


**Fig. 3** Sample 4 (AMDRY 9625/graphite) as-coated: (1) Metal matrix, (2) graphite nodules, and (3) brittle phases (source BIAS)

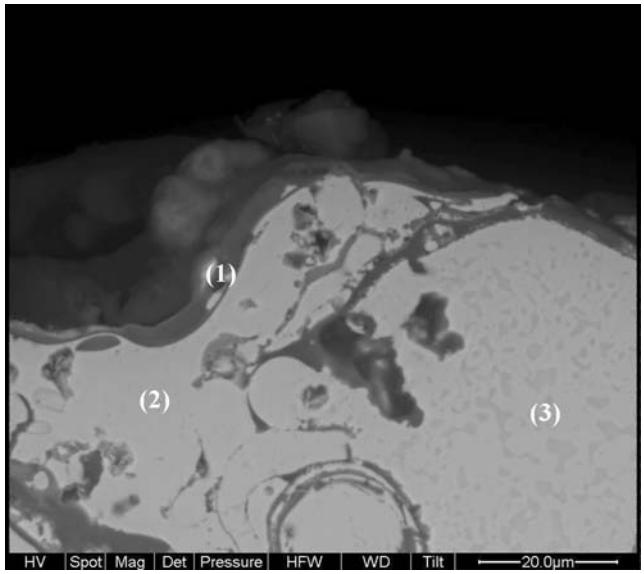


**Fig. 4** Sample 2 after 1100 °C for 1000 h: 3000× BSE micrography of sample in section shows: (1) $Al_2O_3$ protective layer, (2) Metal matrix of CoNiCrAlY depleted in Al, and (3) Metal matrix

samples is about 940 ± 45 μm. Figure 3 shows the back scattered electron (BSE) image of NiCrAlY with added graphite after the laser cladding deposition process (Sample 4). The coating shows a multiphase structure. X-ray diffraction analysis shows the presence of a γ-Ni (c.f.c.) solid solution, a nickel-aluminum intermetallic phase, γ′-$Ni_3Al$ (c.f.c.), and graphite (hex.); small amounts of nickel, $Ni_3C$ (rhomb.), and chromium, $Cr_3C_2$ (orth.) and $Cr_7C_3$ (orth.), carbides are also detected. Very small amounts of oxides, α-$Al_2O_3$ (alumina type; rhomb.), $Y_2O_3$ (cubic), $Cr_2O_3$ (rhomb.), and Ni(Cr, Al)$_2O_4$ (cubic), are also observed, probably due to surface oxidation. The SEM/EDAX analysis (Fig. 3) suggests the presence of a metallic matrix (the lighter phase, Fig. 3(1)) with embedded graphite nodules (the black ones, Fig. 3(2)) and precipitates rich in chromium (the gray ones, Fig. 3(3)), which being brittle phases should improve the abradability of the metal matrix. The thickness of the coating is about 1000 ± 40 μm. The resulting hardness value is about 86 ± 5 HR 15Y.

TBC systems with different top coat porosity show an average thickness of about 1800 μm for all the sprayed coatings. As shown in some previous papers, three kinds of samples were made with different top coat porosity levels (Ref 6, 7). Hardness (HR 15Y) values were found to be 87 ± 4 for Sample 5, 84 ± 2 for Sample 6, and 83 ± 4 for Sample 7.

### 3.2 High-Temperature Oxidation and Thermal Fatigue Behavior

According to OEM specifications, composite coatings must support HTO tests while TBCs must withstand FCT. Samples 1, 2, and 3 coated with CoNiCrAlY and alumina showed a similar behavior when oxidized at high temperatures. A micrograph of the cross section of Sample 2 near the surface after 1000 h at 1100 °C is shown in Fig. 4.

After the oxidation a continuous dark layer formed as shown in Fig. 4. EDAX analysis suggests the formation of an $Al_2O_3$ layer (Fig. 4(1)). It is also possible to observe the presence of a beta phase at the bottom of the micrograph (Fig. 4(3)) and the presence of a beta phase-depleted zone (Fig. 4(2)) between the zone rich in aluminum and the alumina layer as EDAX analysis confirmed. CoNiCrAlY coatings typically exhibit a two-phase microstructure β + γ. The presence of γ increases the ductility of the coating thereby improving the thermal fatigue resistance. As for β-NiAl coatings, high-temperature exposure resulted in a depletion of Al in the zones near the interface of both the TGO (thermally grown oxide) and the substrate by interdiffusion. As the amount of Al decreases, the β-phase tends to dissolve. For this reason, this phase is often described as an aluminum reservoir, and the coating life is often measured in terms of β depletion (Ref 12). The large amount of Al in the AMDRY 995 metal matrix allowed the formation of a protective alumina layer, which slowed down the diffusion of the oxygen through the coating. Figure 5 shows the back scattered electron (BSE) micrograph of the cross sections of the AMDRY 9625 cladded with graphite after 1100 °C for 1000 h. Figure 5 shows the presence of two layers (a lighter one, Fig. 5(1) and a darker one Fig. 5(2)) at the top of the coating. X-ray diffraction analysis suggests that the oxide layers consist essentially of aluminum oxide, α-$Al_2O_3$, and spinel type oxide, Ni(Cr,Al)$_2O_4$; very small amounts of $Cr_2O_3$ and $Y_2O_3$ were also observed. It has to be pointed out that graphite was not detected in the depth explored by the x-ray beam, while the other matrix phases were still observable. Figure 5 also shows the presence of

chromium-rich phases and also the absence of the graphite nodules as observed by x-ray diffraction analysis. No relevant variation in the microstructure after oxidation was observed in comparison with the as-coated samples. As mentioned previously, according to the applied OEM specifications, the minimum requested number of thermal cycles to pass the thermal cycling fatigue test is 250 cycles. All the tested samples passed the FCTs despite the different levels of the top coat porosity (Ref 6, 7).

### 3.3 Abradability Test Results

The abradability test results are summarized in Table 1. The test on an Inconel 718 bare blade at a low incursion rate (Test 1) produced a very high blade wear and transfer of blade material to the shroud. Similar results to the MCrAlY/graphite tests were produced against a c-BN-tipped blade producing partial cutting/smearing of the shroud in the same condition (Test 2) with removal of the tip. Transfer of shroud material to the blade tip, as indicated by a negative overall wear value, arose at maximum incursion conditions with cutting/smearing of the shroud (Test 3). Testing at mid-incursion conditions (50 μm/s) produced localized blade wear and rupture of the shroud (Test 4).

The test against an Inconel 718 bare blade at an incursion rate of 5 μm/s (Test 5) produced a very high blade wear and transfer of blade material to the shroud. By contrast, a c-BN-tipped blade produced cutting/smearing of the shroud under the same conditions (Test 6). At maximum incursion condition, the blade was bent by the incursion process. Transfer of shroud material to the blade tip happened at minimum incursion conditions with cutting/smearing of the shroud (Test 6). Testing at mid-incursion conditions produced localized blade wear and rupture of the shroud (Test 8).

Abradability tests were also performed on thick and porous TBC against a c-BN-tipped blade. The sample with low top coat porosity showed very high blade wear and transfer of blade material to the shroud (Tests 10 and 12). For mid-incursion conditions (Test 11), it was possible to observe a lower blade wear. The samples with medium and high top coat porosity in the three different test conditions (Tests 13-18) all show a slight blade wear, with only little difference between them. Figure 6 shows a comparison of the rub paths produced in the low and high porosity thick, porous TBCs.

Composite coatings (Samples 2 and 4) resulted in being too tough, showing cutting/smearing of the shroud or/and localized blade wear and rupture of the shroud coating during the abradability tests. The TBC with a low porosity level (Sample 5) resulted to be too dense to have good abradability characteristics. Thick and porous TBC systems with medium (Sample 6) and high porosity (Sample 7) levels of the top coat showed a good abradability against tipped blades. The tests showed a low blade wear and no shroud coating rupture.

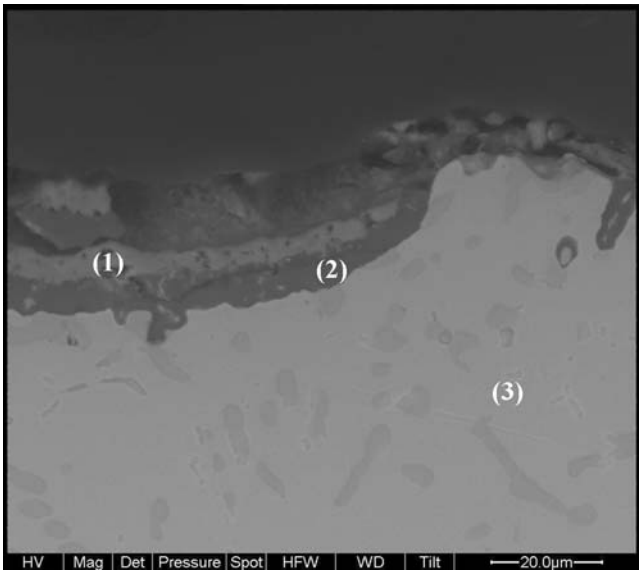


**Fig. 5** Sample 4 (AMDRY 9625/graphite) after 1000 h at 1100 °C: (1) $NiAl_2O_4$ layer, (2) $Al_2O_3$ protective layer, and (3) Metal matrix with embedded brittle phases

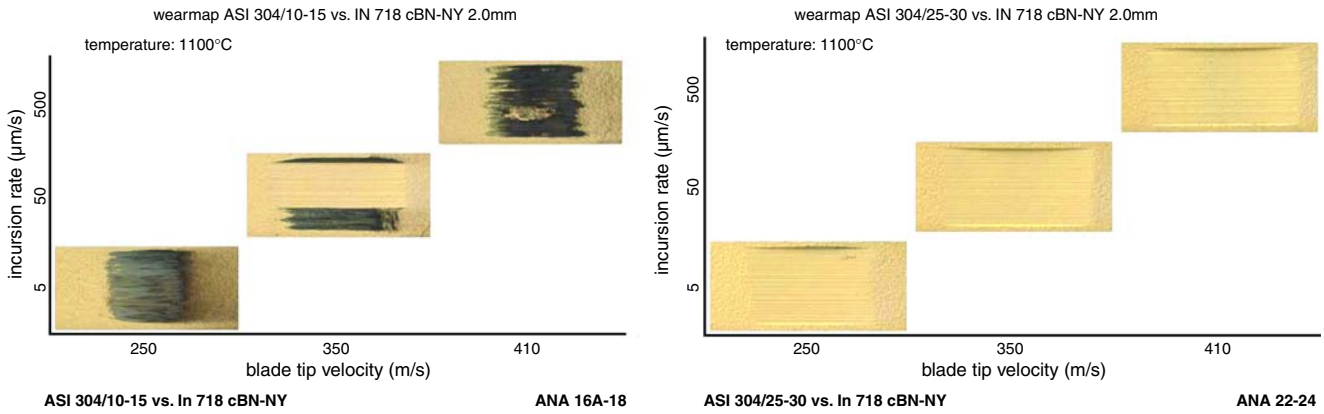


**Fig. 6** Appearance of rub paths produced by three different test conditions in low porosity (left) and high porosity (right) thick TBCs with c-BN-tipped blades. Dark rub path appearance is indicative of blade material transfer to the coating

## 4. Conclusions

New composite metal-ceramic coatings were developed and tested as possible high-temperature resistance abradable materials for the first stage of industrial gas turbines. APS deposition process was used to obtain high-temperature resistant composite CoNiCrAlY/$Al_2O_3$ coatings. Composite CoNiCrAlY/Graphite coatings were produced by laser cladding. The HTO behavior of the composite coatings was studied. CoNiCrAlY/$Al_2O_3$ and CoNiCrAlY/graphite coatings after 1000 h at 1100 °C do not show relevant microstructural modifications. The oxidation resistance of the new composite coatings satisfied OEM specifications. The newly developed thick and porous TBC systems passed the thermal fatigue test according to the considered OEM procedures, regardless of the top coat porosity. Hardness Rockwell 15Y measurements suggest that all the produced coatings must be used with abrasive-tipped blades. MCrAlY/graphite and MCrAlY/alumina shrouds were generally too resistant to cutting or resulted in an extensive material transfer to the c-BN-tipped blades. Thick and porous TBC coatings with top coats having medium and high porosity levels have shown good abradability behavior against c-BN-tipped blades.

### Acknowledgment

The present work was supported by ABRANEW project RS0098 (FP5 Programme).

### References

1. Y. Tamarin, *Protective Coatings for Turbine Blades*, ASM International, Materials Park, OH, 2002
2. M. Dorfman, U. Erning, and J. Mallon, Gas Turbines Use 'Abradable' Coatings for Clearance-Control Seals, *Seal. Technol.*, 2002, **2002**(1), p 7/8
3. 2003 NASA Seal/Secondary Air System Workshop (2003), Nov 5-6, Ohio Aerospace Institute, Cleveland, OH
4. F. Ghasripoor, R. Schmid, and M. Dorfman, Abradables Improve Gas Turbine Efficiency, *Mater. World*, 1997, **5**(6), p 328-330
5. M.P. Boyce, *The Gas Turbine Engineering Handbook*, 2nd ed., Gulf Professional Publishing, Houston, TX, 2001
6. A. Scrivani, G. Rizzi, and C.C. Berndt, Enhanced Thick Thermal Barrier Coatings that Exhibit Varying Porosity, *Mater. Sci. Eng. A*, 2008, **476**(1-2), p 1-7
7. A. Scrivani, G. Rizzi, U. Bardi, C. Giolli, M. Muniz Miranda, S. Ciattini, A. Fossati, and F. Borgioli, Thermal Fatigue Behavior of Thick and Porous Thermal Barrier Coatings Systems, *J. Therm. Spray Technol.*, 2007, **16**(5-6), p 816-821
8. H.B. Guo, R. Vaβen, and D. Stöver, Thermophysical Properties and Thermal Cycling Behavior of Plasma Sprayed Thick Thermal Barrier Coatings, *Surf. Coat. Technol.*, 2005, **192**(1), p 48-56
9. J.R. Davis, et al., *Handbook of Thermal Spray Technology*, ASM International, Materials Park, OH, 2005
10. L. Lutterotti, S. Matthies, and H.R. Wenk, MAUD (Material Analysis Using Diffraction): A User Friendly JAVA Program for Rietveld Texture Analysis and More, *Proceedings of the 12th International Conference on Textures of Materials (ICOTOM-12)*, J.A. Szpunar, Ed., NRC Research Press, Ottawa, 1999, **1**, p 1599-1604
11. R. Schmid and A.R. Nicoll, Advance in Abradable Coatings for Gas Turbines, *Proceedings of International ASME Gas Turbine and Aeroengine Congress and Exposition*, June 13-16, 1994 (The Hague, Netherlands), 1994
12. R. Sivakumar and B.L. Mordike, High Temperature Coatings for Gas Turbine Blades: A Review, *Surf. Coat. Technol.*, 1989, **37**(2), p 139-160